

A Molecular Blueprint at the Apical Surface Establishes Planar Asymmetry in Cochlear Hair Cells

Basile Tarchini,^{1,*} Christine Jolicoeur,¹ and Michel Cayouette^{1,2,3,*}

¹Cellular Neurobiology Research Unit, Institut de recherches cliniques de Montréal (IRCM), Montreal, QC H2W 1R7, Canada

²Département de Médecine, Université de Montréal, Montreal, QC H3T 1J4, Canada

³Department of Anatomy and Cell Biology, and Division of Experimental Medicine, McGill University, Montreal, QC H3A 0G4, Canada

*Correspondence: basile.tarchini@ircm.qc.ca (B.T.), michel.cayouette@ircm.qc.ca (M.C.)

<http://dx.doi.org/10.1016/j.devcel.2013.09.011>

SUMMARY

Sound perception relies on the planar polarization of the mechanosensory hair cell apex, which develops a V-shaped stereocilia bundle pointing toward an eccentric kinocilium. It remains unknown how intrinsically asymmetric bundles arise and are concomitantly oriented in the tissue. We report here that *mlnsc*, *LGN*, and *G α i* proteins, which classically regulate mitotic spindle orientation, are polarized in a lateral microvilli-free region, or “bare zone,” at the apical hair cell surface. By creating and extending the bare zone, these proteins trigger a relocalization of the eccentric kinocilium midway toward the cell center. *aPKC* is restrained medially by *mlnsc/LGN/G α i*, resulting in compartmentalization of the apical surface that imparts the V-shaped distribution of stereocilia and brings the asymmetric bundle in register with the relocalized kinocilium. *G α i* is additionally required for lateral orientation of cochlear hair cells, providing a possible mechanism to couple the emergence of asymmetric stereocilia bundles with planar cell polarity.

INTRODUCTION

The establishment and maintenance of polarity is critical for the function and survival of essentially all cells. One striking example in mammals is found in the sensory epithelium of the cochlea, where mechanosensory hair cells (HCs) perceive sounds through microvilli-derived stereocilia at their apical surface (AS). HCs display two levels of planar polarity. First, intrinsic polarity is defined as a vector running from the cell center toward the eccentric primary cilium, or kinocilium, that is located at the vertex of the V-shaped bundle of stereocilia. Second, HCs are uniformly oriented in the cochlea, their planar vectors aligned with the mediolateral axis of the organ of Corti, a coiled ribbon bearing one row of inner hair cells (IHCs) and three rows of outer hair cells (OHCs). This concerted tissue orientation is referred to as planar cell polarity (PCP) (Goodrich and Strutt, 2011) and, together with cell-intrinsic asymmetry, is crucial for HC function, as only stereo-

cilia deflections along the mediolateral axis can efficiently modulate electric currents in HCs (Shotwell et al., 1981).

By embryonic day 14.5 (E14.5) in the mouse, prospective HCs are postmitotic but still morphologically undifferentiated. The first evidence of planar polarity occurs when, driven by an unknown mechanism, the kinocilium shifts away from the center of the HC to a roughly lateral position, followed by preferential growth of nearby microvilli into stereocilia (Cotanche and Corwin, 1991; Denman-Johnson and Forge, 1999; Tilney et al., 1992). Because intrinsic asymmetry and tissue orientation are thus established together and interlocked, the existence of two levels of HC polarity remained unclear until analyses of mouse mutants for homologs of “core” PCP genes in invertebrates. Reminiscent of misoriented wing hairs or body bristles in fly mutants, mouse PCP mutants show mild to randomized HC orientation defects depending on the gene, HC subtype, or cochlear region (Curtin et al., 2003; Lu et al., 2004; Montcouquiol et al., 2003; Wang et al., 2005, 2006). Kinocilia still shift to the HC periphery, but their positions are no longer uniformly lateral and foreshadow HC misorientation before bundles become detectable. Importantly, PCP mutant HCs have a largely intact apical morphology, suggesting that HC cytoskeleton asymmetry is not instructed by core PCP signaling but relies on different molecular effectors that are largely unidentified.

This dual polarity system intriguingly stands apart from other tissues where PCP operates. Indeed, besides uncoordinated cell orientation, single-cell asymmetry is often also defective in PCP mutants. Primary cilia fail to shift and tend to remain central in node cells, leading to beating and left-right patterning defects (Antic et al., 2010; Borovina et al., 2010; Hashimoto et al., 2010; Song et al., 2010). The distal hair is mispositioned centrally in fly wing cells (Wong and Adler, 1993), and basal body rootlets fail to orient uniformly within one multiciliated cell (Guirao et al., 2010; Mitchell et al., 2009; Tissir et al., 2010; Vladar et al., 2012). How is HC intrinsic asymmetry established, then, if not by PCP? The centrifugal shift of the basal body giving rise to the kinocilium is required, as impairing ciliogenesis induces a circular stereocilia bundle in a subset of HCs where the basal body remains central (Jones et al., 2008). However, although the kinocilium is considered a lever for PCP signaling inside the HC that guides the orientation of the bundle in the tissue, there is no evidence that the peripheral kinocilium or basal body instruct V-shaped asymmetrical stereocilia distribution at the AS. Polarized stereocilia bundles still arise in HCs lacking a kinocilium,

even when orientation of the shifted basal body is uncoupled from the bundle vertex (Jones et al., 2008; Sipe and Lu, 2011). Thus, it remains unknown how the mechanosensory compartment acquires its functional asymmetry and how this process is interlocked with HC orientation in the tissue.

Given their ability to couple cortical polarity with the cytoskeleton, we set out to investigate whether proteins involved in mitotic spindle orientation might play a role in the planar polarization of HCs. In *Drosophila* neuroblasts, proliferation and cell fate depend on coupling mitotic spindle orientation with cortical polarity, thereby ensuring asymmetric inheritance of fate determinants between sister cells. At prometaphase, the polarity proteins Par-3 and aPKC asymmetrically localize at the apical cortex, where they recruit the adaptor protein Inscuteable (Insc), which in turn binds Partner of Inscuteable (Pins) and the heterotrimeric G protein $G\alpha i$ (Kraut et al., 1996; Parmentier et al., 2000; Schaefer et al., 2000, 2001; Schober et al., 1999; Wodarz et al., 1999, 2000; Yu et al., 2000). Together, these proteins recruit effectors pulling on astral microtubules to position the mitotic spindle, a role widely conserved across tissues exhibiting oriented cell division (Morin and Bellaïche, 2011). LGN, a mammalian homolog of Pins, is a scaffolding protein that directly binds mammalian Insc (mInsc) via its N-terminal tetratricopeptide motifs and $G\alpha i$ via its C-terminal Goloco domains (Yuzawa et al., 2011; Zhu et al., 2011). LGN is recruited to the cell cortex by $G\alpha i$ (Du and Macara, 2004), and promotes planar divisions in the vertebrate neuroepithelium, but perpendicular divisions in other contexts (El-Hashash et al., 2011; Konno et al., 2008; Morin et al., 2007; Peyre et al., 2011; Williams et al., 2011). mInsc functions as a tissue-specific adaptor for apicobasal divisions in the neuroepithelium (Postiglione et al., 2011; Zigman et al., 2005), and is sufficient to reorient planar divisions vertically (Konno et al., 2008; Poulson and Lechler, 2010).

In this study, we focus on a neglected apical HC compartment uniquely devoid of microvilli or stereocilia. This “bare zone” appears between the shifted kinocilium and the lateral cell junctions, and hosts the polarized localization of mInsc, LGN, and $G\alpha i$. These proteins collectively extend the AS to create the bare zone, leading to a secondary relocation of the shifted kinocilium toward the cell center. mInsc/LGN/ $G\alpha i$ exclude aPKC from the bare zone, and the resulting compartmentalization of the HC apex acts as a blueprint to define the V-shaped contour of the stereocilia bundle and to bring it in register with the relocated kinocilium. $G\alpha i$ is also required for HC orientation in the cochlea, likely participating in PCP signaling to influence the early kinocilium shift. Therefore, interaction between LGN and $G\alpha i$ is a candidate mechanism to couple the emergence of an asymmetric bundle with orientation cues in the tissue, illuminating how the mechanosensory compartment is streamlined for perception in the ear.

RESULTS

mInsc/LGN/ $G\alpha i$ Are Planar Polarized at the HC Apical Surface

Immunostaining of mouse cochlea sections at birth revealed that mInsc/LGN/ $G\alpha i$ are enriched apically in HCs, with a lateral bias (Figures 1A–1C). En face views showed that these proteins form a thick crescent lateral to the stereocilia bundle at the AS

(Figures 1D–1F). Pattern specificity was verified using cochlea electroporation and organotypic culture, where fusion proteins were similarly localized, unlike the Egfp control (Figure 1G). LGN overlapped both with surface microtubules that are polarized laterally, and the lateral portion of the cuticular plate, the actin-dense structure supporting the stereocilia (Figures 1H and 1I). The LGN medial boundary precisely matched the emergence of the tallest row of stereocilia (Figure 1H, arrowheads). Lateral to the bundle, only a small AS region around the base of the kinocilium was deprived of LGN protein (Figure 1H, arrow). mInsc and $G\alpha i$ shared a similar subcellular distribution (schematized in Figure 1H'). Interestingly, the lateral HC region where mInsc/LGN/ $G\alpha i$ are localized stands out, as it is devoid of microvilli, unlike the medial surface (Figure 1J). Although similarly polarized along the mediolateral axis, the pattern of mInsc/LGN/ $G\alpha i$ is very distinct from PCP proteins, which are polarized at cell junctions but absent from the HC surface (Deans et al., 2007; Montcouquiol et al., 2006; Wang et al., 2005, 2006).

mInsc/LGN/ $G\alpha i$ Are Molecular Markers of a Microvilli-Free Zone Emerging during Apical HC Morphogenesis

Epithelial cells in the sensory epithelium are generally covered with microvilli, except for the vicinity of the central primary cilium (Figure 2A), which in prospective IHCs shifts laterally at E15.5 (Figure 2B). Labeling microvilli and young stereocilia with an antibody against phosphorylated Ezrin/Radixin/Moesin (pERM) revealed a microvilli-free zone forming lateral to the shifted kinocilium (Figure 2C). The formation and extension of this “bare zone” followed the base-to-apex and mediolateral gradients of HC differentiation along the cochlea (Figures 2D–2F; McKenzie et al., 2004). Interestingly, the shifted kinocilium was often in close proximity to the HC junction, but appeared to recede toward the HC center with the emergence and extension of the intervening bare zone (Figures 2B and 2C; see also Figures S4C and S4D available online). This suggests that kinocilium placement is the product of (1) a roughly lateral shift that first brings it in close contact with the cell junction, and (2) an inward relocation under the influence of the growing bare zone, which brings it midway between the lateral junction and the cell center. Accordingly, HC basal bodies from which the kinocilium nucleates adopted less eccentric positions in progressively more differentiated HCs after the early shift (Figure 2G). We thus propose that the bare zone is created de novo between the shifted kinocilium and the lateral HC junction, as the AS is rounding up from an initially hexagonal shape.

mInsc/LGN/ $G\alpha i$ distribution at the HC apex precisely coincided with the bare zone in time and space, with LGN first detected in the lateral region where pERM staining disappeared in E15.5 IHCs (Figure 2H). Like the bare zone, the LGN domain appeared and grew following the differentiation gradient (Figures 2I–2K), with an initially narrow apicolateral crescent that extended to the base of the stereocilia (compare Figures 2H and 2K). In costainings, LGN matched the region devoid of pERM signal (Figure 2L). This early asymmetric enrichment was similar for mInsc and $G\alpha i$ (data not shown). Therefore, mInsc/LGN/ $G\alpha i$ are bona fide molecular markers of the bare zone. Early LGN crescents appeared approximately at the time of the kinocilium shift (Figures 2I–2K), but the two were only in loose spatial register, often displaying distinct planar orientations (Figure 2M,

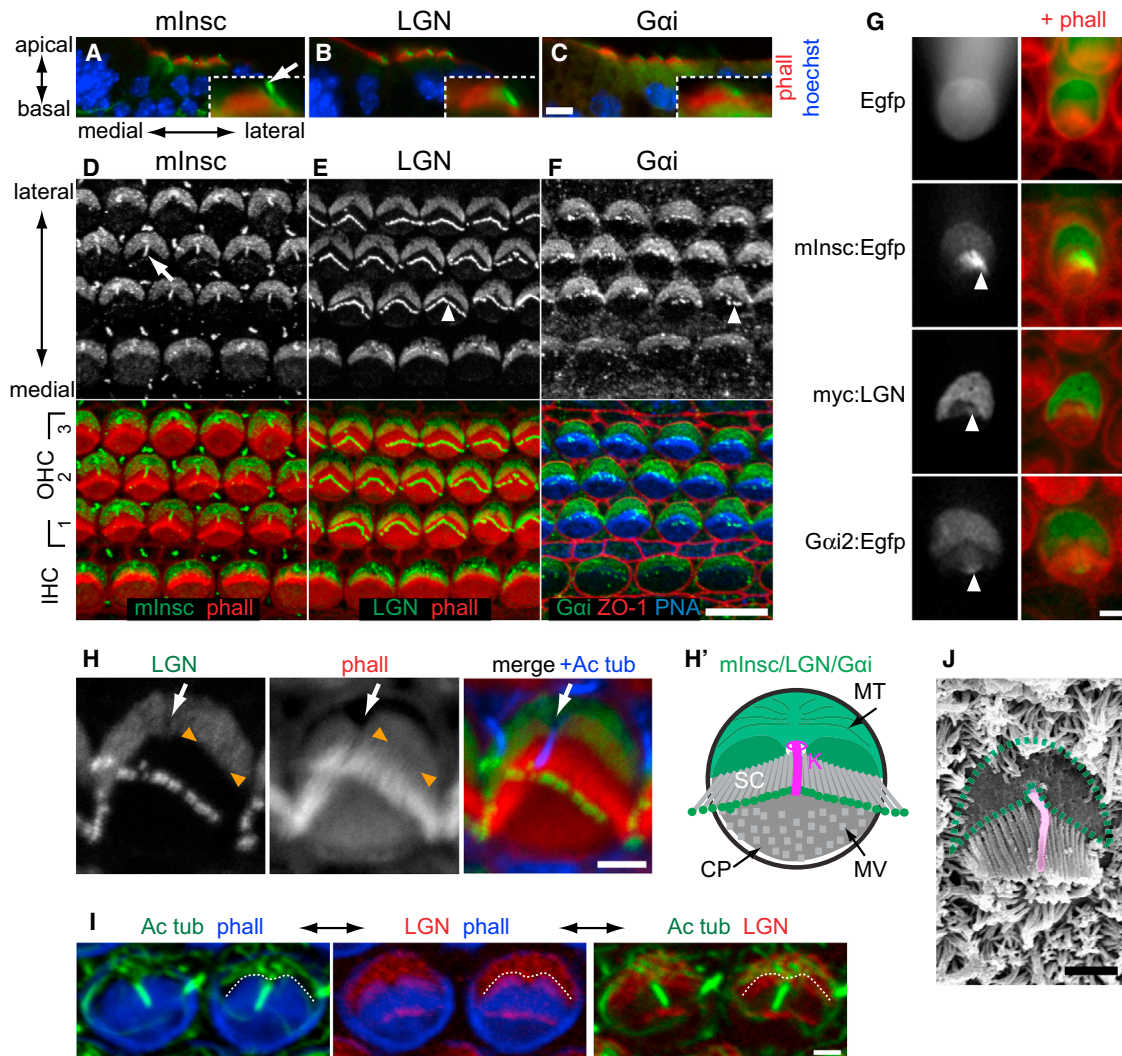


Figure 1. mInsc/LGN/Gai Proteins Are Polarized Lateral to the Stereocilia Bundle at the HC Apex

(A–C) Immunostains for mInsc, LGN, and *Gai* (green) on P0 cochlea sections with the F-actin marker phalloidin (phall; red) and the DNA dye Hoechst (blue). Insets show a magnification of the lateral-most OHC3. Kinocilium labeling by the mInsc antibody (arrow in A and D) is unspecific, and retained in *mInsc* mutants (see Figure S2D).

(D–F) Surface view of P0 organ of Corti immunostained for mInsc, LGN, and *Gai*. Bottom panels show merge with either phalloidin, or ZO-1 (apical cell junctions) and peanut agglutinin (PNA, stereocilia bundle). Beside their polarized distribution at the lateral AS, LGN and *Gai* are also enriched at stereocilia tips (arrowheads).

(G) OHCs electroporated with the indicated protein fusions. Arrowheads show enrichment in the bundle distinct from the AS.

(H) LGN medial boundary precisely coincides with lateral settling of stereocilia at the AS (arrowheads), and LGN is absent from a small AS region surrounding the base of the kinocilium, labeled by acetylated tubulin (Ac tub; arrow). LGN pattern is schematized in (H'). MT, apical microtubules; K, kinocilium; SC, stereocilia; MV, microvillus; CP, cuticular plate. P2 OHC.

(I) LGN covers both surface microtubules (green) and the portion of the cuticular plate (blue) lateral to the bundle. Hatched line depicts boundary between surface microtubules and the cuticular plate. E18.5 OHCs.

(J) The AS region where mInsc/LGN/*Gai* are localized (dotted line) is devoid of microvilli, as illustrated by scanning electron microscopy at birth. Kinocilium is highlighted in pink. P0 IHC.

Scale bars: 10 μ m (A–F), 2 μ m (G–J). See also Figure S1.

2N, and 2P). However, further differentiation brought the kinocilium and bare zone in register, with the kinocilium emerging exactly at the center of the mInsc/LGN/*Gai* crescent (Figures 2O and 2P), as seen around birth (Figures 1H and 1I). Consequently, bare zone proteins are unlikely candidates to trigger the centrifugal shift of the kinocilium, but they likely participate in the relocalization of the kinocilium (Figure 2Q).

At the tissue level, mInsc/LGN/*Gai* labeled the only regions of the whole sensory epithelium lacking microvilli (Figures 1J and 2A–2F), and their asymmetric pattern was limited to HCs, whereas PCP proteins are also polarized apically in supporting cells. mInsc was only transcribed in HCs from E14.5 (Figures S1A, S1B, and S1F–S1H), and although LGN was more ubiquitously transcribed, the protein was only detected and planar

polarized at the HCs apex (Figures S1C–S1E and S1I–S1J). Altogether, by defining a polarized surface devoid of microvilli, *mlnsc*/LGN/*Gai* could help define intrinsic asymmetry of the apical cytoskeleton in HCs.

***mlnsc* Is Required for Proper Extension of the Bare Zone and Bundle Shape**

To study *mlnsc* function in HCs, an 82kb deletion (*mlnsc*^{DEL}) was created in vivo that encompassed all coding sequences for the short *mlnsc* isoform (Figures S2A–S2C). A putative longer isoform with 47 additional amino acids N-terminal is transcribed from an alternative first exon left intact by the deletion (Figure S2A; Izaki et al., 2006). We detected protein encoded by the long isoform in control, but not *mlnsc*^{DEL} HCs, verifying the specificity of the *mlnsc* antibody and the absence of the long isoform in *mlnsc*^{DEL} (Figure S2D). Other antibodies detecting both short and long *mlnsc* isoforms showed the same protein distribution in controls (data not shown). Although *mlnsc*^{DEL} pups looked normal at birth, and mutant and control cochleas could not be distinguished among littermates, mutant HCs displayed a consistently smaller AS and bundles that appeared more flat (Figures S3A and S3B). Analysis at a later stage (P4) confirmed these results and revealed a specific reduction of the bare zone surface, whereas the complementary medial AS did not vary significantly, arguing against developmental delay at birth (Figures S3C and S3D). In addition, stereocilia formed two distinct sub-bundles in a small subset of HCs, a severe morphological defect never observed in controls (Figure S3E). HC orientation in the tissue was unaffected in *mlnsc*^{DEL} (data not shown). *mlnsc* is thus specifically required for the normal extension of the bare zone where it localizes, and for a properly shaped bundle edge abutting its medial boundary.

LGN Is Essential to Shape the Bundle Contour and Relocalize the Kinocilium

To study LGN function, we raised a mouse line from a Eucomm ES clone where LGN exon 5 is preceded by a reporter and flanked by *loxP* sites (Figures S2E and S2F; *LGN* *betageo*; *flox* or *LGN*^{BF}). The reporter caused an early N-terminal truncation that abolished LGN immunostaining in HCs, hence confirming LGN inactivation and antibody specificity (Figure S2G). As in *mlnsc*^{DEL}, mutant and control cochleas could not be distinguished at birth. Nevertheless, loss of LGN severely disrupted apical morphology in HCs (Figure 3A). Phalloidin stainings and scanning electron microscopy revealed defects increasing in severity from disorganized bundle ultrastructure (type I) to complete loss of cytoskeleton asymmetry (type III; Figures 3B and 3C). In type I HCs, stereocilia placement was very irregular at the lateral bundle edge, and bundles were flattened, like in *mlnsc*^{DEL} (Figure 3B, arrows). In type II HCs, two main sub-bundles emerged at distinct positions, and normally lateral surface microtubules invaded the central and medial regions where the cuticular plate and stereocilia were missing (Figures 3B, 3C, and S4A). Type II HCs were reminiscent of the very abnormal HCs in *mlnsc*^{DEL} (Figure S3E). In type III HCs, surface microtubules were concentrated at the center of the cell, with three or more sub-bundles distributed around the periphery, including laterally where the bare zone normally stands (Figures 3B, 3C, and S4A). The relative proportion of the different mutant HC types showed some variability across animals (Figures 3D

and 3E). Importantly, as seen in *mlnsc*^{DEL}, absence of LGN reduced the HC apex surface (Figure 3F). These results suggest that by establishing an exclusion zone laterally, LGN defines the asymmetric placement of stereocilia above the AS and affects the distribution of surface microtubules and the cuticular plate under the AS.

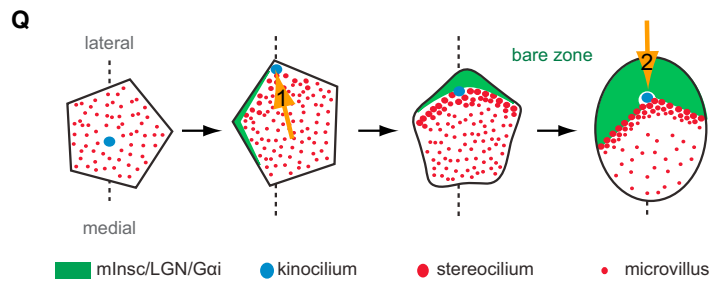
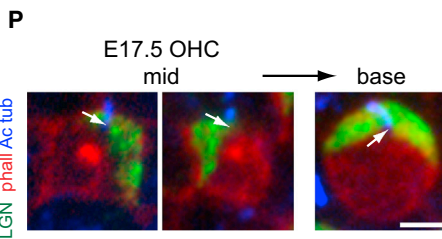
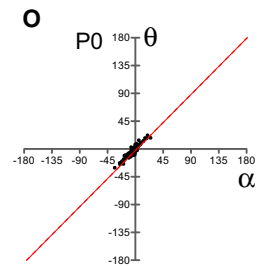
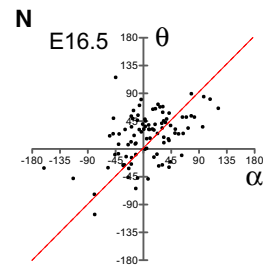
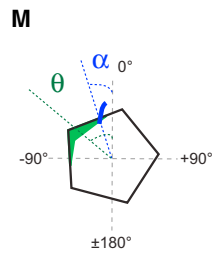
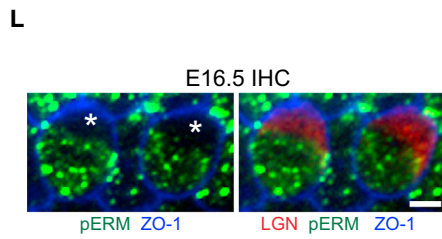
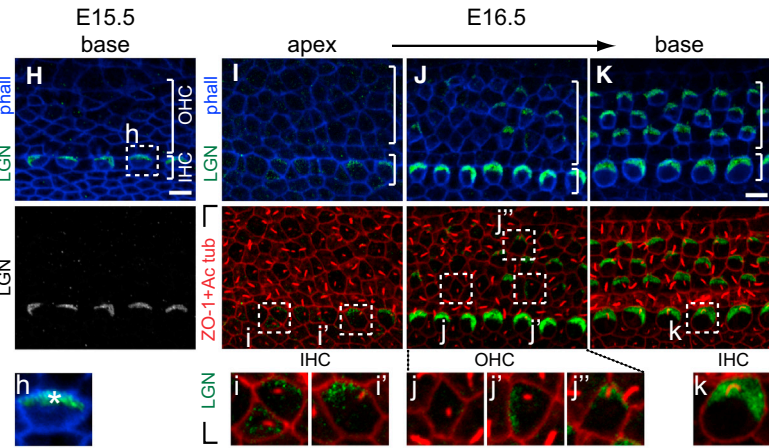
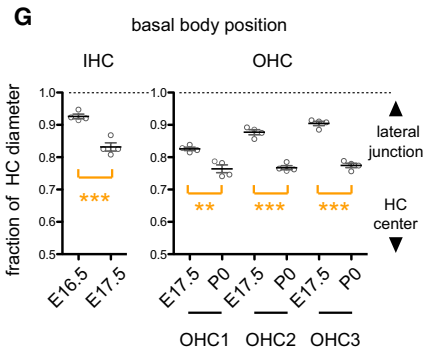
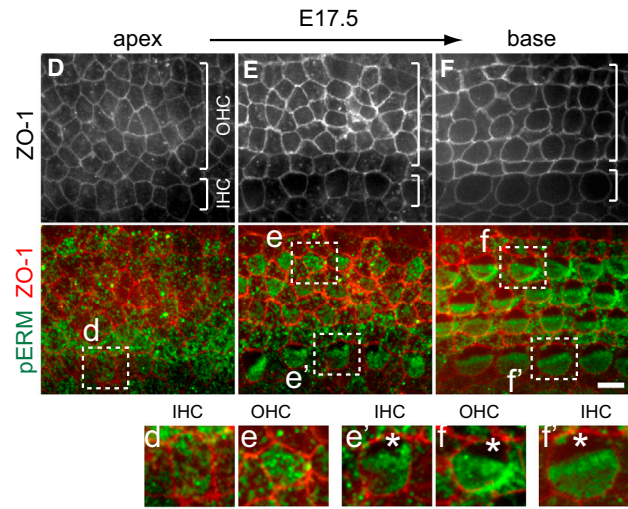
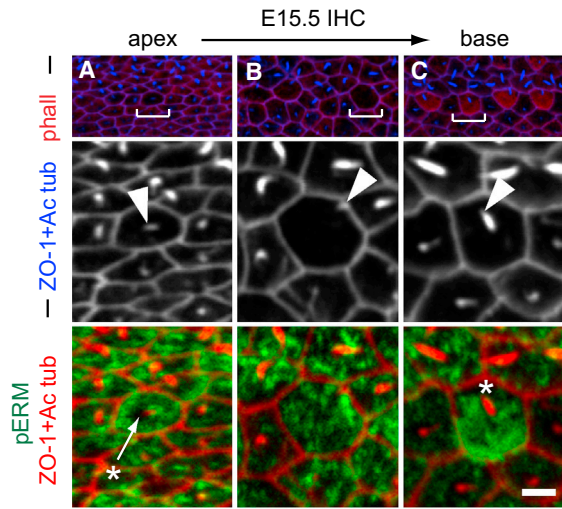
To a lesser extent than intrinsic morphology, HC planar orientation also appeared abnormal in *LGN*^{BF}, as suggested by the misorientation of some cohesive bundles in type I HCs (Figure 3A, arrowhead). To study HC orientation (PCP) without being biased by aberrant bundle morphology, the planar position of the kinocilium was monitored for all HCs in a field at P0. Cumulative plotting revealed abnormally scattered kinocilia in *LGN*^{BF} (Figures 3G and 3H). While control kinocilia were centered and emerged laterally at middistance to the cell junction (see also Figure 2G), mutant kinocilia occupied variably eccentric positions in the lateral half of the AS, being rarely found in the medial half. This contrasts with core PCP mutant HCs, where kinocilia have a normal and constant eccentricity that coincides with normal morphology. Mutant kinocilia were connected to either one of the sub-bundles in OHCs (Figures 3B and S4A), but frequently disconnected from the bundle in IHCs (Figure S4B). In spite of these severe defects at birth, the early lateral shift of the kinocilium occurred normally in *LGN*^{BF} (Figures S4C–S4E), consistent with the LGN protein crescent being initially polarized independently from the kinocilium (Figures 2N and 2P). LGN is therefore unlikely to be part of the PCP machinery that orients the early kinocilium shift (Montcouquiol et al., 2003). By contrast, LGN appears crucial for the subsequent inward relocalization of the kinocilium. As in the context of mitotic spindle orientation, *mlnsc*/LGN/*Gai* could exert force on surface microtubules in order to bring the forming bundle in register with the eccentric kinocilium.

***mlnsc*/LGN/*Gai* Are Interdependent for Their Normal Enrichment at the Bare Zone**

Because *mlnsc*, LGN, and *Gai* form a protein complex to orient the mitotic spindle, we next asked whether they each localized normally in mutant contexts. LGN protein amounts at the bare zone were reduced in *mlnsc*^{DEL} and, reciprocally, *mlnsc* was decreased in *LGN*^{BF} at P0 (Figures 4A–4D). Similarly, *Gai* was downregulated at the bare zone in both *mlnsc* and *LGN* mutant HCs (Figures 4E–4G). These proteins thus generally rely on each other for normal levels of enrichment. This molecular interplay was originally described in fly neuroblasts (Schaefer et al., 2000, 2001; Yu et al., 2000), and together with documented protein interactions (Du and Macara, 2004; Yuzawa et al., 2011; Zhu et al., 2011), suggests that *mlnsc*/LGN/*Gai* similarly form a complex in mouse HCs. Importantly, although downregulated in mutant HCs, partner proteins were still detected, polarized, and likely functional to some degree, as HC defects in *mlnsc*^{DEL} and *LGN*^{BF} showed different severities.

Inactivating *Gai* Disrupts both HC Orientation in the Cochlea and HC Intrinsic Polarity

At least two of the three *Gai* mouse genes, *Gai2* and *Gai3*, were expressed in purified HCs as detected by RT-PCR (Figure S5A), and *Egfp* fusions of the three proteins, but not closely related *Gai0*, were similarly enriched at the bare zone (Figure S5B). Thus, to circumvent expected functional redundancy, we



(legend on next page)

used Pertussis toxin (PTX) to inactivate G protein signaling. We first established that coimmunoprecipitation of mycLGN with *Gai2*:Egfp was severely impaired by a construct encoding the PTX catalytic subunit (PTXa), probably because the toxin sequesters *Gai* in the inactive $G\alpha\beta\gamma$ complex (Figure S5C). PTXa was then expressed specifically in single HCs by electroporating E14.5 cochleas with a construct carrying an *Atoh1* enhancer/ β -globin promoter (*Atoh1-PTXa*), and apical morphology was analyzed after 6 days in culture (Figure S5D; see [Experimental Procedures](#)). We predicted that PTXa would affect bare zone complex enrichment and reduce the HC apex, as seen in *mlnsc* and *LGN* mutants. Indeed, all *PTXa*-electroporated HCs had a strong decrease of endogenous LGN and *mlnsc* (Figure S6A and data not shown), and lost the lateral enrichment of coelectroporated *Gai2*:Egfp (Figure S6B). The AS was also reduced compared to control electroporations (Figure S6C). However, *PTXa* caused unique and severe HC orientation (PCP) defects as monitored by kinocilium planar orientation (Figures S6D–S6F). To verify that the phenotypes could be accounted for by *Gai*, we designed distinct sets of shRNAs against *Gai2* and *Gai3* (Figures S6G and S6H), and electroporated them in cochlea explants. Individually, potent shRNAs against either *Gai2* or *Gai3* at most reduced the LGN crescent (Figures S6I and S6J). By contrast, simultaneous knockdown of both *Gai2* or *Gai3* in the same HC phenocopied the *PTXa* results, with severe LGN loss and drastic HC misorientation (Figures S6I and S6J).

To dissect *Gai* function, we generated transgenic mice carrying the *Atoh1-PTXa* construct. Transgenics at E18.5 could not be distinguished from wild-type littermates, likely due to *Atoh1*-restricted *PTXa* expression. Since all *PTXa*-electroporated HCs consistently showed severely reduced LGN in explants, we used LGN as a readout of *PTXa* expression. Incomplete transgene expression resulted in a mosaic of affected and unaffected HCs in the organ of Corti, and we used HCs expressing normal LGN as internal controls (Figure 5A; see [Experimental Procedures](#)). Coordinated orientation in the field (PCP) first appeared abolished in *PTXa* OHCs, with a randomized profile of angle distri-

bution based on kinocilia positions, whereas IHCs were less affected (Figures 5B and 5C). Interestingly however, overall randomization reflected distinct outcomes across rows: kinocilia in OHC1 seemed inverted, with angles around $\pm 180^\circ$ (Figure 5D), whereas OHC2 and OHC3 kinocilia encompassed more variable angles but were generally positioned at the medial and lateral HC surface, respectively. Therefore, orientation defects follow an increasing OHC3 to OHC1 gradient of severity. Together, these results indicate that generally lateral HC orientation controlled by the direction of the early kinocilium shift requires *Gai*, but not *mlnsc* or *LGN*, suggesting that *Gai* could interpret PCP signaling.

In addition, *PTXa* HCs displayed defects in cell-intrinsic polarity similar to *mlnsc* and *LGN* mutants. The bare zone was almost absent in *Atoh1-PTXa* HCs, with microvilli/stereocilia and the underlying cuticular plate occupying most of the reduced AS (Figures 5E and 5F). Surface microtubules were polarized, following the aberrant orientation of the kinocilium (Figure 5G), but invaded central regions where the cuticular plate was missing in HCs with multiple sub-bundles (Figure 5H), as seen in *LGN^{BF}* (Figure S4A). Kinocilia were abnormally close to cell junctions (Figures 5D, 5E, and 5I) as observed only transiently during normal HC differentiation (Figures 2A and 2G), suggesting that the bare zone is needed for the inward relocalization process. Again, defects were increasingly pronounced from OHC3 to OHC1, and IHCs were less affected (Figures 5A, 5I, and 5J and data not shown). Altogether, by (1) binding LGN/*mlnsc* to create the bare zone and (2) interpreting PCP information to guide the early kinocilium shift, *Gai* is a good candidate to couple the intrinsically asymmetric distribution of stereocilia, surface microtubules, and the cuticular plate with orientation cues in the tissue that use the kinocilium as a lever in the HC.

The HC Apical Surface Undergoes Axial Compartmentalization Independently from PCP Signaling

Core PCP proteins segregate in antagonistic modules located on opposite sides of the cell membrane (Goodrich and Strutt, 2011).

Figure 2. LGN Is a Marker of the Microvilli-Free Region Emerging Laterally during Apical HC Morphogenesis

(A–C) Immunostains for phosphorylated ezrin/radixin/moesin (pERM) in the E15.5 cochlea. Bottom panels show alternate channel magnifications of a prospective IHC indicated by brackets in the top panel. Arrowheads indicate the kinocilium, and asterisks the microvilli-free regions (bare zone in C) defined by the absence of pERM staining.

(D–F) Progressive emergence of the bare zone in increasingly differentiated HCs from the apex to the base of a E17.5 cochlea. IHCs lack a bare zone in apex regions (D), but have one in the more developed basal regions (E', F', asterisk). OHCs follow the same progression, with a delay (E and F, asterisk).

(G) Basal body position at the HC apex at the stages indicated, expressed as a fraction of the mediolateral cell diameter, where 0.5 is the cell center and 1 the lateral junction. Graphs represent mean \pm SEM for four samples where pericentrin-labeled basal body position was measured for HCs in a field at the base of the cochlea. ** $p < 0.01$, *** $p < 0.001$; unpaired Student's t test.

(H) LGN protein is first detected at E15.5 in IHCs and already localized in a crescent (asterisk).

(I–K) Progressive onset of LGN apical enrichment from the apex to the base of an E16.5 cochlea. Prospective HCs only very transiently show unpolarized LGN localization (i, bottom HC; see also Figure S1D). LGN asymmetric enrichment generally coincides with the kinocilium shift (compare top and bottom HCs in I, and J with J' and J'').

(L) LGN localization overlaps with the bare zone, as revealed by absence of pERM staining (asterisk).

(M) Reference system used to measure the planar orientation of the kinocilium (blue; α) and the center of the LGN crescent (green; θ). 0° angle is a perfectly lateral orientation.

(N and O) Angular register between the kinocilium and the LGN crescent in E16.5 (N) and P0 (O) OHCs. Plotted points represent single OHCs with the kinocilium orientation (α) in x and the LGN crescent orientation (θ) in y. The red line indicates perfect register. 95 (N) and 92 (O) OHCs from four different samples are shown.

(P) LGN crescent (green) and the kinocilium (blue, arrows point to the base) only adopt a perfect register along with HC differentiation, as illustrated by comparing localization between less (mid cochlea position) and more (base position) mature E17.5 OHCs.

(Q) Schematic representation of early apical morphogenesis comparing bare zone protein distribution with cytoskeletal landmarks at the HC apex. Arrows "1" and "2" depict the early shift and subsequent inward relocalization of the kinocilium, respectively. Scale bars: 2 μ m (A–C, L, and P), 5 μ m (D–F and H–K). See also Figures S2 and S3.

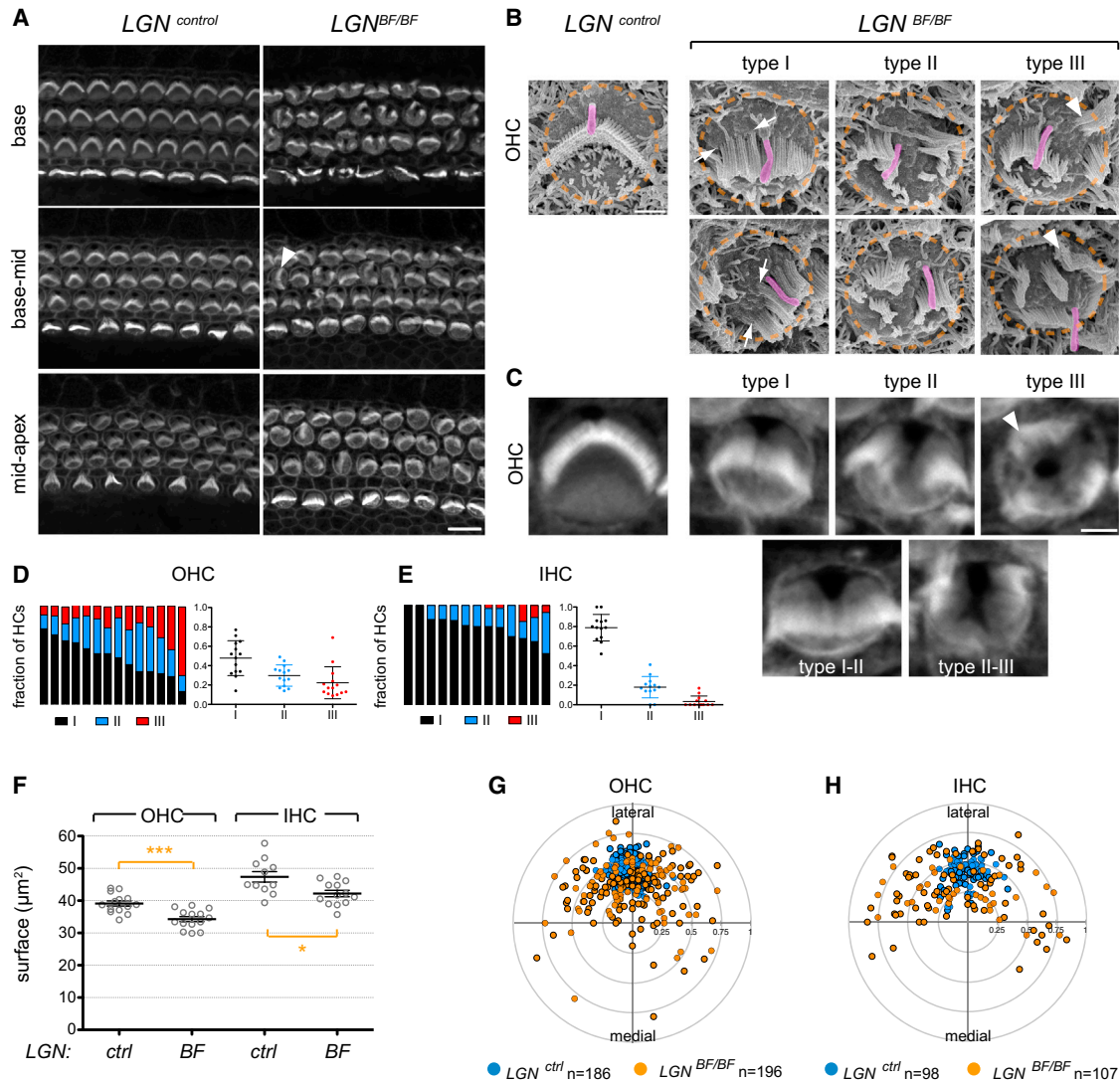


Figure 3. Defective Stereocilia Placement and Kinocilium Relocalization in *LGN^{BF}* Mutants at Birth

(A) Phalloidin stainings of the organ of Corti at 3 positions along the apicobasal axis of the cochlea. OHCs with a single bundle are sometimes misoriented (arrowhead).

(B and C) Scanning electron microscopy (B) and fluorescent (phalloidin; C) views of OHC examples representing graded phenotype severity at the cochlea base (type I less affected > type III more affected). Stereocilia settling at the lateral bundle edge is very irregular in type I HCs (B, arrows). Type III HCs have sub-bundles laterally where the bare zone is normally found (B and C, arrowheads). Cell boundary is outlined and the kinocilium is highlighted in pink (B). Bottom panels in (C) show intermediate examples between type I-II and II-III HCs.

(D and E) Proportions of each severity type at the cochlea base in 14 (OHCs) and 12 (IHCs) *LGN^{BF}* samples (fraction \pm SD).

(F) The HC apical surface is significantly reduced in *LGN^{BF}* HCs (OHCs: -12.4% , $p = 0.0002$, $n = 14$ controls and mutants; IHCs: -10.9% , $p = 0.0109$; $n = 11$ controls and 13 mutants). Graph shows mean \pm SEM. * $p < 0.05$, *** $p < 0.001$, unpaired Student's t test.

(G and H) Polar plots of kinocilium position at the AS obtained from four different samples. Scale bars: 10 μm (A), 2 μm (B and C). See also Figures S2 and S4.

At HC/supporting cell junctions, core PCP proteins are enriched in either medial or lateral subdomains. At the hair cell apex, *mInsc/LGN/G α i* are restricted to the lateral bare zone, raising the question whether complementary medial proteins exist. While investigating candidates, we observed that aPKC was polarized medially at the AS (Figure 6A). Three different antibodies showed similar protein distribution, and antibody specificity was controlled using a shRNA against aPKC ζ (Figures S7A and S7B). aPKC colabeling with *mInsc* and *LGN* revealed close surface complementarity between aPKC medially and

the bare zone laterally in the same HC (Figures 6B and 6C). The lateral bundle edge sat at the interface (Figure 6D; see also Figure 1H). Interestingly, Par-3 was localized at the bare zone (Figure 6E), and complementary to aPKC (Figure 6F). A Par-3 fusion protein electroporated in cochlea explants confirmed enrichment lateral to the bundle (Figure S7C).

We next asked how aPKC distribution is achieved during HC differentiation. At E15.5 in IHCs and E16.5 in OHCs, aPKC covered the AS in *LGN*-negative HCs, but was downregulated laterally in more differentiated, *LGN*-positive HCs (Figures

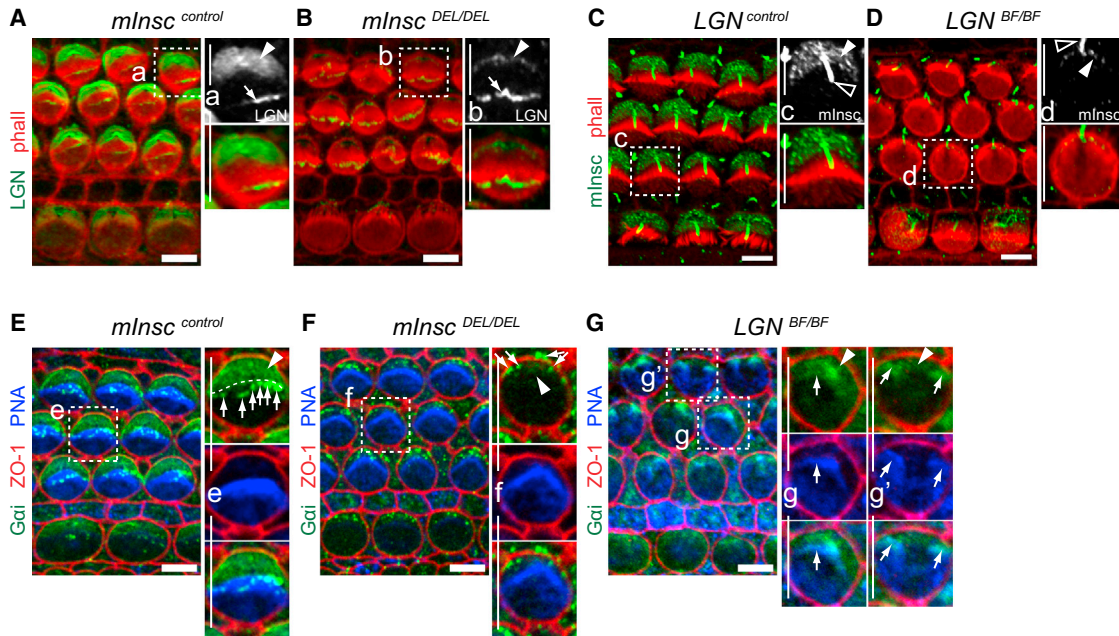


Figure 4. *mInsc*/LGN/*Gai* Are Interdependent for Proper Enrichment at the Bare Zone

(A and B) LGN enrichment is reduced but still detectable at the bare zone (arrowheads) of *mInsc^{DEL}* HCs. Arrows indicate LGN at the tips of stereocilia.

(C and D) *mInsc* enrichment is reduced but still detectable at the bare zone (arrowheads) of *LGN^{BF}* HCs. Kinocilium labeling is unspecific (open arrowheads; see Figure S2D).

(E–G) *Gai* at the bare zone (arrowheads) is downregulated but still detectable in both *mInsc^{DEL}* (F) and *LGN^{BF}* (G). While unchanged in *mInsc^{DEL}* stereocilia (F, arrows), *Gai* loses its specificity for tips and localizes to the whole defective bundle in *LGN^{BF}* (G, arrows), an extra source of antibody signal that should not obscure decreased protein levels at the bare zone (G, arrowheads). Magnified and split channel views of boxed HCs are shown on the right of each main panel. Scale bars: 5 μm.

7A–7D). Moreover, the region of aPKC exclusion coincided with the spatial extent of LGN (Figures 7A–7D) and the bare zone defined by absence of pERM (Figure S7D) at all stages and cochlea levels analyzed. This suggests that aPKC localization is antagonized by *mInsc*/LGN/*Gai*. Consistently, aPKC localized normally until birth in *mInsc^{DEL}* HCs, but invaded the reduced bare zone around P1 (Figure 7E). aPKC was still excluded from both the base of stereocilia and the kinocilium in *mInsc^{DEL}*, showing selective ectopic localization only where *mInsc*/LGN/*Gai* are normally present (Figures 7F and 7G). In *LGN^{BF}*, aPKC invaded the lateral AS, but from earlier stages (Figures 7H and 7I). Similarly, aPKC was ectopically found past the bundle in *PTXa*-expressing HCs, irrespective of cell orientation in the field (Figure 7J). Two distinct axial compartments are thus defined by the segregation of polarity proteins at the AS, with *mInsc*/LGN/*Gai* acting in part to exclude aPKC at the bare zone. Unlike aPKC, however, Par-3 distribution was largely unchanged in *mInsc* and *LGN* mutant HCs (data not shown). By analogy with fly neuroblasts, where *mInsc*/LGN/*Gai* homologs are recruited by Par-3 via binding to *Insc* (Schober et al., 1999; Wodarz et al., 1999), Par-3 might thus function as a localization cue in HCs. Supporting this possibility, murine Par-3 and *mInsc* proteins interacted directly in a cell-free pull-down assay (Figure S7E).

Using the *Vangl2^{LP}* allele, we tested the prediction that both AS protein modules should be intact in a core PCP mutant, in which HCs with compromised orientations retain normal intrinsic polarity. *mInsc*/LGN and aPKC were normally enriched at the bare

zone and the complementary AS compartment in misoriented *Vangl2^{LP}* HCs, respectively (Figures S8A–S8C). Conversely, in both *mInsc^{DEL}* and *LGN^{BF}* organs of Corti, the asymmetric enrichment pattern of the core PCP proteins *Dvl2* and *Fz6* was similar to controls (Figures S8D–S8G). Therefore, polarity proteins at the AS and core PCP proteins represent two largely independent polarity systems.

The Bare Zone Complex Excludes aPKC and Stereocilia to Shape the Bundle at the HC Apex

Addressing aPKC and Par-3 function proved difficult, likely because their function at apical junctions is crucial to create and maintain the AS, an obstacle to address a further role in planar patterning. We thus undertook a gain-of-function approach to establish the importance of lateral (*mInsc*/LGN/*Gai*) versus medial (aPKC) protein localization on stereocilia distribution at the HC apex. Crumbs (Crb) localizes at the AS in epithelial cells, and as expected, a *Crb3:venus* protein was enriched at the HC apex without planar polarization (Figure 8A). Consequently, a *Crb3:myc:Gxi2* fusion localized more uniformly than *Gxi* alone, and drastically extended endogenous LGN from a lateral crescent to the whole apex (Figure 8B). Remarkably, *Crb3:myc:Gxi2* conversely restricted aPKC to a central domain bearing an abnormally constrained and rounded brush of stereocilia/microvilli (Figure 8C). A *Crb3:myc:LGN* construct had the same effect on aPKC and bundle shape, as expected from extended endogenous LGN localization in *Crb3:myc:Gxi2* HCs (Figure 8D). Importantly, *Crb3* without the *Gxi* moiety did not extend LGN domain or result in

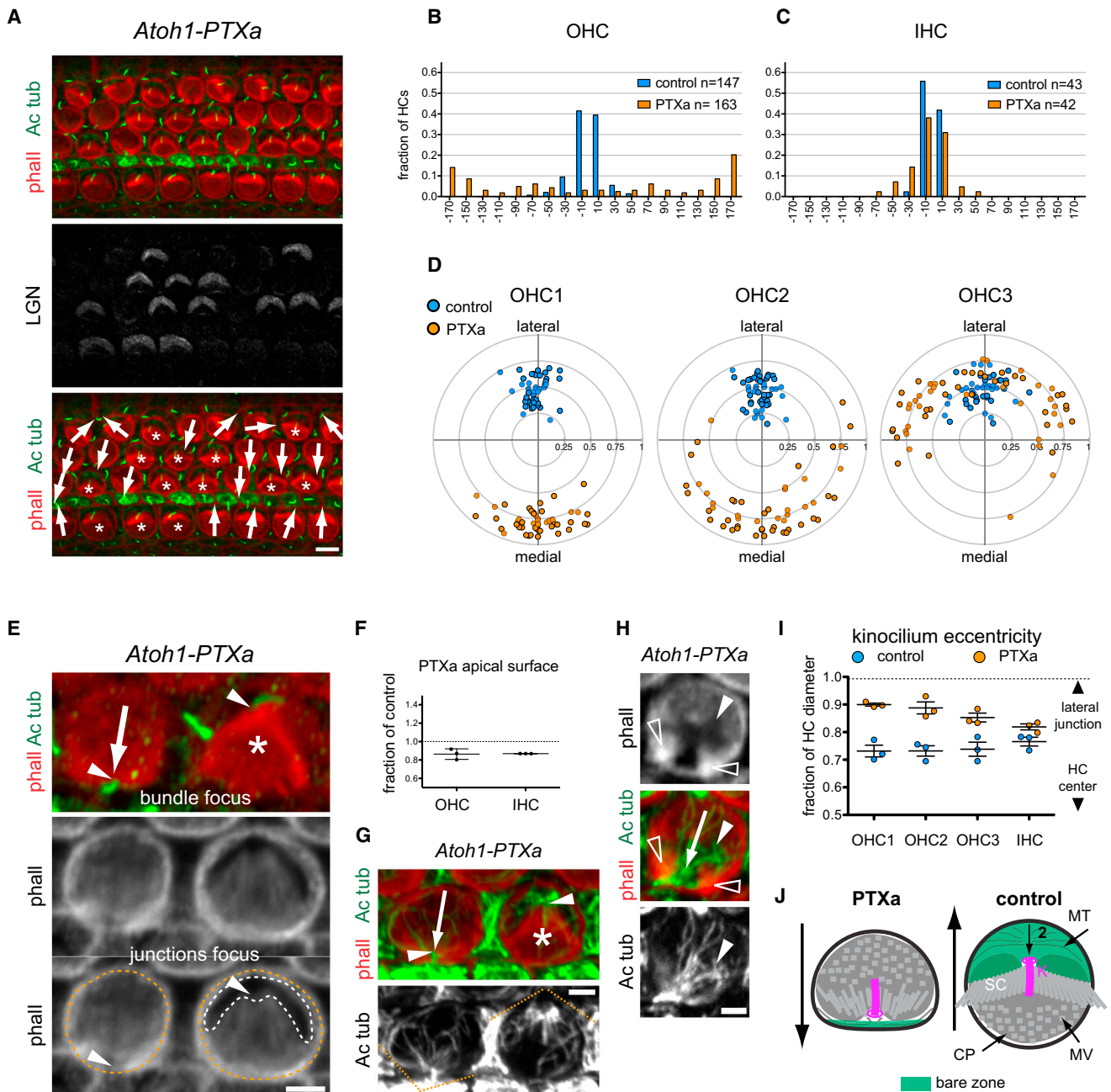


Figure 5. Pertussis Toxin Affects both HC Orientation and HC Intrinsic Asymmetry In Vivo

(A) Incomplete *Atoh1-PTXa* transgene expression results in a mosaic of affected (associated arrows, defective LGN enrichment) and unaffected (asterisks, normal LGN enrichment) HCs in the E18.5 organ of Corti. HC planar orientation based on kinocilium position (green) is indicated by the direction of the arrow for each affected HC.

(B and C) Frequency distribution of HC orientation. PTXa and control HCs are respectively LGN-negative and LGN-positive HCs in the same field in 3 transgenic samples at the cochlea base (n = 147 control OHCs, 162 PTXa OHCs, 43 control IHCs, 42 PTXa IHCs).

(D) Polar plots of kinocilium position by OHC row for the cells graphed in (B).

(E) Close-up on adjacent affected (left, associated arrow) and unaffected (right, asterisk) OHC1s. Arrow indicates inverted orientation of the affected HC based on the kinocilium position (arrowheads). Affected cells have smaller apices (outlined in orange), and the much reduced bare zone coincides with an abnormally eccentric kinocilium (arrowhead). The portion of the bare zone devoid of F-actin is outlined in white.

(F) AS in affected HCs expressed as a fraction of control HCs in the same field (n = 3; mean ± SEM).

(G) Same general description as in (E). In most affected HCs, acetylated tubulin-labeled surface microtubules are still polarized (orange brackets) and follow the orientation of the HC given by the kinocilium (arrowheads).

(H) In some affected cells with multiple sub-bundles (hollow arrowheads), surface microtubules invade more central HC regions where the phalloidin-labeled cuticular plate is defective (arrowheads), as also observed in LGN mutant HCs (Figure S4A). Arrow indicates HC orientation as in (E) and (G).

(legend continued on next page)

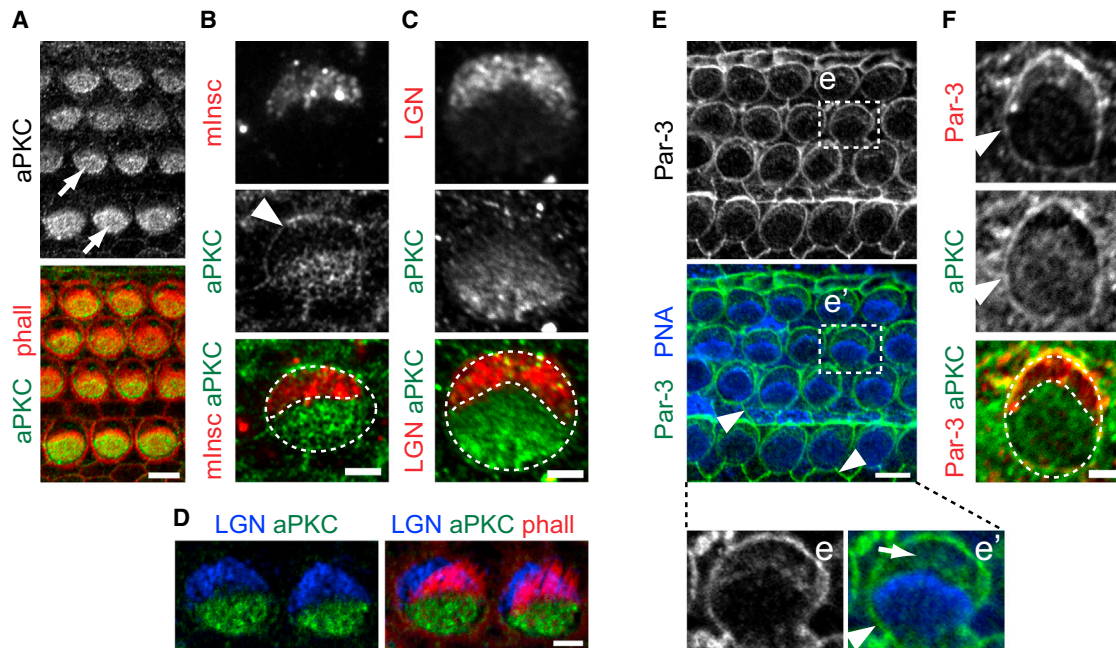


Figure 6. aPKC Defines a Medial Compartment Complementary to mlnc/LGN/G α i and Par-3 at the HC Apex

(A) aPKC is polarized medially at the AS (arrows) in P0 HCs.

(B and C) Colabeling of mlnc (B, E17.5 IHC) and LGN (C, P4 IHC) with aPKC.

(D) The stereocilia bundle (red) emerges from the lateral-most portion of the aPKC-positive AS.

(E) Par-3 is polarized lateral to the bundle (PNA, blue) at the AS at P0 (arrow). The boxed HC is magnified in the bottom panels for each channel view (E and E').

(F) Colabeling of Par-3 and aPKC (E18.5 OHC). In (B), (C), and (F), single channels are shown separately with the merge at the bottom, and HC boundary and the border between the bare (lateral) and medial zones are outlined. Arrowheads indicate aPKC (B and F) or Par-3 (E and F) at apical junctions. Scale bars: 5 μ m (A and E), 2 μ m (B–D, F). See also Figure S7.

constrained aPKC or bundles. Along with ectopic aPKC distribution in bare zone mutants, these results suggest that mlnc/LGN/G α i limit aPKC medially to create a molecular blueprint for cytoskeleton asymmetry at the HC apex, notably defining the contour of the growing stereocilia bundle (Figure 8E).

DISCUSSION

In this study, we uncover a function for mlnc/LGN/G α i that is unrelated to the control of mitotic spindle orientation, cell fate, or tissue organization. Studying HC morphological differentiation in the mouse cochlea after proliferation has ended, we show that these proteins guide the planar polarization of the apical cytoskeleton.

Early Kinocilium Shift and Planar Cell Polarity

Following on the analogy with spindle orientation, we first envisioned that the early crescent of mlnc/LGN/G α i could recruit effector proteins to pull on surface microtubules and trigger the centrifugal shift of the kinocilium. While mlnc/LGN/G α i become polarized at E15.5 and generally coincide with eccentric kinocilia, this hypothesis proved improbable. First, protein crescents at the HC apex seem ill-suited to exert planar forces for a

side translation of the kinocilium, which would be expected to involve proteins enriched at apical junctions. Second, the protein crescent and the shifted kinocilium often adopt distinct orientations, with the kinocilium at the very edge of the protein domain. Third, none of the functional insults to mlnc, LGN or G α i prevented the centrifugal shift of the kinocilium, although inactivating G α i, but not LGN, led to drastic HC misorientation. Therefore, we conclude that, while it does not trigger the shift per se, G α i influences its general direction. Interestingly, PTXa does not randomize HC orientation, with OHC1 being cleanly inverted, raising the possibility that instead of providing an orientation cue, G α i could participate in the elusive readout of PCP protein asymmetry. HCs kinocilia can indeed shift toward or away from the same core PCP protein when comparing cochlear and vestibular HCs, or HCs located on opposite sides of the line of polarity reversal in the vestibule (Deans et al., 2007; Wang et al., 2006). A model in which G α i does not strictly assume a PCP function is supported by comparing polarity proteins at the AS (this study) and PCP proteins at apical junctions. While both groups form opposite modules along the mediolateral axis and their protein members rely on each other for normal enrichment (this work and Deans et al., 2007; Montcouquiol

(I) Kinocilium placement at the HC apex expressed as a fraction of the cell diameter, where 0.5 is the cell center and 1 the lateral junction (mean \pm SEM; n = 3).

(J) Cartoon of PTXa and control OHC1 shown in (E) and (G). The secondary relocation of the kinocilium is indicated with the arrow "2". MT, microtubules; SC, stereocilia; CP, cuticular plate; MV, microvillus. Scale bars: 5 μ m (A), 2 μ m (E, G, and H). See also Figures S5 and S6.

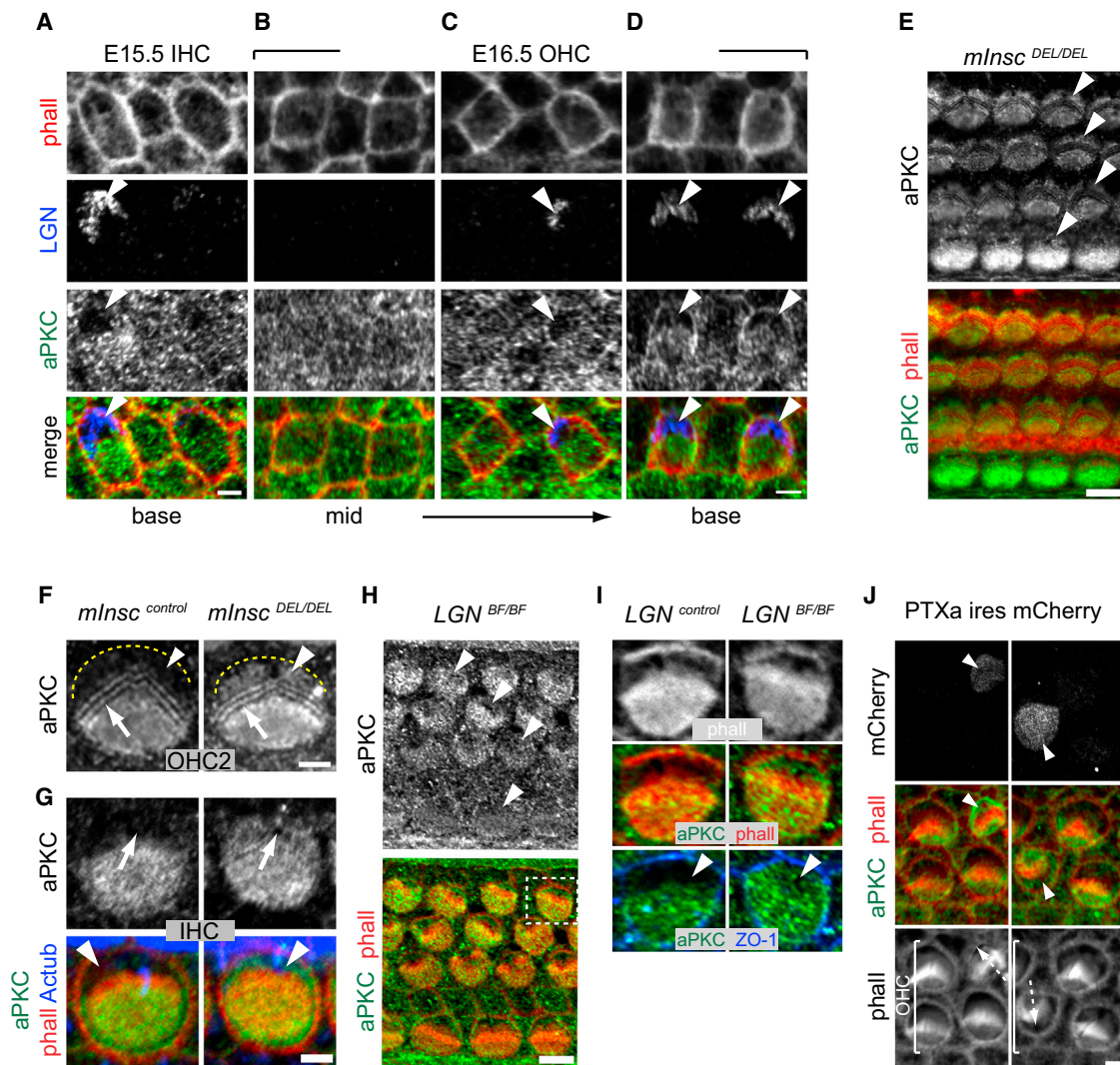


Figure 7. aPKC Is Excluded from the Lateral HC Surface by *mInsc/LGN/Gαi*

(A–D) Early during differentiation, HCs downregulate aPKC at the emerging bare zone (arrowheads) labeled by LGN. Note how less differentiated HCs with little or no LGN enrichment still have lateral aPKC staining (right IHC in A, both OHCs in B, and left OHC in C).

(E) aPKC becomes ectopically localized laterally (arrowheads) at P1 in *mInsc^{DEL}*.

(F and G) Close-up views of P1 OHCs (F) and IHCs (G). The position of the lateral HC junction is indicated by the dotted line (F). aPKC is abnormally enriched at the bare zone (arrowheads) in *mInsc^{DEL}*, but still absent from the base of both stereocilia (F, arrow) and the kinocilium (G, arrow).

(H and I) aPKC already invaded the bare zone at E18.5 in *LGN^{BF}* (arrowheads). Magnified and alternate channel views of boxed OHC in (H) shown in (I; right).

(J) aPKC loses its AS restriction in *PTXa*-electroporated HCs from cochlea explants cultured for 6 days (arrowheads). Electroporated HC orientation is indicated by an arrow. Note how aPKC is found on both sides of the bundle irrespective of HC orientation. Scale bars: 5 μm (E and H), 2 μm (A–D, F, G, I, and J).

et al., 2006; Vladar et al., 2012; Wang et al., 2005, 2006), they seem to be largely independent, as judged by normal protein distribution in reciprocal mutant contexts.

In *mInsc/LGN/Gαi* mutant contexts, partner proteins fail to be enriched at proper levels, yet cell-intrinsic defects are ranging in severity from reduced (*mInsc^{DEL}*) to absent (*PTXa*) bare zone, and from misaligned stereocilia edge (*mInsc^{DEL}; LGN^{BF}* type I) to complete loss of bundle asymmetry (*LGN^{BF}* type III; *PTXa*). Besides being unequally required for common tasks, the unique role of *Gαi* in HC orientation also indicates that these proteins can exert distinct functions, despite their colocalization and physical interactions.

Bare Zone Formation and Kinocilium Inward Relocalization

We report here a detailed description of the lateral portion of the HC apex deprived of microvilli or stereocilia and its origin, notably by identifying *mInsc/LGN/Gαi* as molecular markers. Concomitantly, we discover that, as the HC apex grows and becomes rounded, the shifted kinocilium undergoes a relocalization from a lateral position close to the HC junctions to a more central position. In *PTXa* HCs, where *mInsc/LGN/Gαi* fail to be enriched and a region devoid of microvilli is virtually absent, the kinocilium remains closely juxtaposed to the junction. Based on these observations, we propose that *mInsc/LGN/Gαi* are

required for adding apical membrane lateral to the shifted kinocilium, thereby creating the compartment we call the bare zone, and relocalizing the kinocilium on the medial side of the *mlnsc/LGN/G α i* crescent (Figure 8F). *mlnsc/LGN/G α i* appear well suited to superimpose the apical cytoskeleton with the cortical domain they define at the AS, possibly using traction on surface microtubules to corral, balance and maintain the basal body/kinocilium at the vertex of the forming bundle. Accordingly, in *LGN* mutant HCs, surface microtubules lose their crescent restriction and kinocilia adopt a wide range of lateral positions, emerging at variable distances from the HC center. PTXa HCs show the same defects, but kinocilia and surface microtubules are overall more consistently eccentric, suggesting that while *G α i* uniquely influences the early shift, it has a less prominent role than *LGN* in kinocilium relocalization. Conversely, mildly imprecise orientation observed in *LGN^{BF}* HCs is likely explained by improper kinocilium relocalization and/or maintenance following the normal early shift.

A Blueprint of Complementary Proteins at the Apical Surface

Our data indicate that the HC apex becomes compartmentalized in the mediolateral axis during differentiation (Figure 8F). This model is strengthened by the complementary medial and lateral localization of aPKC and Par-3, which are known to function with *mlnsc/LGN/G α i* in the regulation of spindle orientation. Bare zone proteins negatively regulate aPKC localization since its lateral exclusion is lost in *mlnsc/LGN/G α i* mutant contexts, and forced extension of the bare zone complex constrains the aPKC domain. Of note, ectopic aPKC in the bare zone is only detected late in *mlnsc* mutants, but occurs earlier in *LGN* mutants, possibly contributing to the more severe defects observed in *LGN^{BF}*. Interestingly, exclusion of *LGN* from the mitotic cell apex is required to secure planar divisions and was reported to depend on aPKC in some but not other epithelial cell types (Bergstralh et al., 2013; Guilgur et al., 2012; Hao et al., 2010; Peyre et al., 2011; Zheng et al., 2010). As mutating the serine in *LGN* identified as an aPKC target in MDCK cysts (Hao et al., 2010) failed to alter mycLGN distribution at the HC apex (data not shown), it remains unclear whether aPKC reciprocally regulates bare zone protein localization.

aPKC was reported to progressively exclude Par-3 from the AS in some epithelia, limiting it to apical junctions (Afonso and Henrique, 2006; Martin-Belmonte et al., 2007; Morais-de-Sá et al., 2010; Walther and Pichaud, 2010). Therefore, the lateral bare zone might represent a special kind of apical compartment where Par-3 is retained via the absence of aPKC. In the HC medial domain as in many other epithelial types, aPKC enrichment at the AS might contribute to microvilli assembly by recruiting and activating ezrin, a scaffolding protein required for normal microvilli development in enterocytes (Saotome et al., 2004; Wald et al., 2008).

Interestingly, we also observed asymmetrical enrichment of both aPKC and Par-3 at apical junctions, with the same respective mediolateral bias as the HC apex (data not shown and Figure S7C). Although a detailed characterization of aPKC/Par-3 localization at the junctions was beyond the scope of this study, an interesting possibility is that their junctional localization could

help spread a PCP-related signal to the HC apex, linking the polarity of the two compartments. In this respect, Par-3 is a candidate to orient the early *mlnsc/LGN/G α i* crescent independently from the kinocilium because its enrichment at the AS is not dependent on the bare zone complex.

The Bare Zone and Asymmetric Stereocilia Distribution at the HC Apex

Proteins known to regulate stereocilia formation have been primarily identified by mapping deafness genes in humans, and most are localized in the stereocilia proper or in interstereociliary and stereokinociliary links, promoting stereocilia differentiation, growth, and integration/maintenance into a bundle (Richardson et al., 2011). Here, in contrast, we propose that there is also a blueprint for the distribution of stereocilia at the HC surface, at the time when the differentiation process is only starting in elected microvilli. Compartmentalized polarity proteins at the AS guide both the asymmetric organization of the cytoskeleton under the AS (the surface microtubules and the cuticular plate) and above the AS (stereocilia, kinocilium) (Figure 8F). Our data specifically indicate that *mlnsc*, *LGN* and *G α i* create a sharp microvilli exclusion boundary as a strategy to define the V-shaped contour of the stereocilia bundle (Figure 8F). Classic anatomical studies did not comment on the bare zone, but noted how the lateral edge of the bundle, which is initially circular, progressively becomes semicircular and then V-shaped in mammals (Kaltenbach et al., 1994; Zine and Romand, 1996). These changes in bundle contour clearly mirror the absence, first appearance, and changing medial boundary of the bare zone proteins. Although phenotype severity varies in *mlnsc*, *LGN*, and PTXa mutants, the bare zone surface and the bundle edge are systematically affected, culminating in the ectopic growth of stereocilia on the lateral HC apex in *LGN* and PTXa mutants. Such major insults to bundle asymmetry likely account for hearing impairment in human syndromes recently associated to *LGN* mutations (Doherty et al., 2012; Walsh et al., 2010; Yariz et al., 2012). Interestingly, the medial edge of the bundle is defined days after the lateral edge, when microvilli unintegrated into the bundle disappear after birth (Zine and Romand, 1996). Therefore, medial and lateral bundle edges are implemented through radically different processes, an additional asymmetry at the HC apex that could be relevant to the establishment of graded heights across stereocilia rows.

In summary, we propose that *mlnsc/LGN/G α i* simultaneously establish the asymmetrical distribution of differentiating stereocilia at the HC apex and use traction on surface microtubules to reposition and center the kinocilium in the middle of the bare zone, at the vertex of the forming bundle (Figure 8F). Because the direction of the early kinocilium shift is controlled by PCP signaling and *G α i* to impart a roughly lateral HC orientation in the tissue, *mlnsc/LGN/G α i* are uniquely positioned to both create and align intrinsic bundle asymmetry with tissue polarity during early HC differentiation.

EXPERIMENTAL PROCEDURES

Mice

All animal work was carried out in accordance with the Canadian Council on Animal Care guidelines and approved by the IRCM Animal Care Committee.

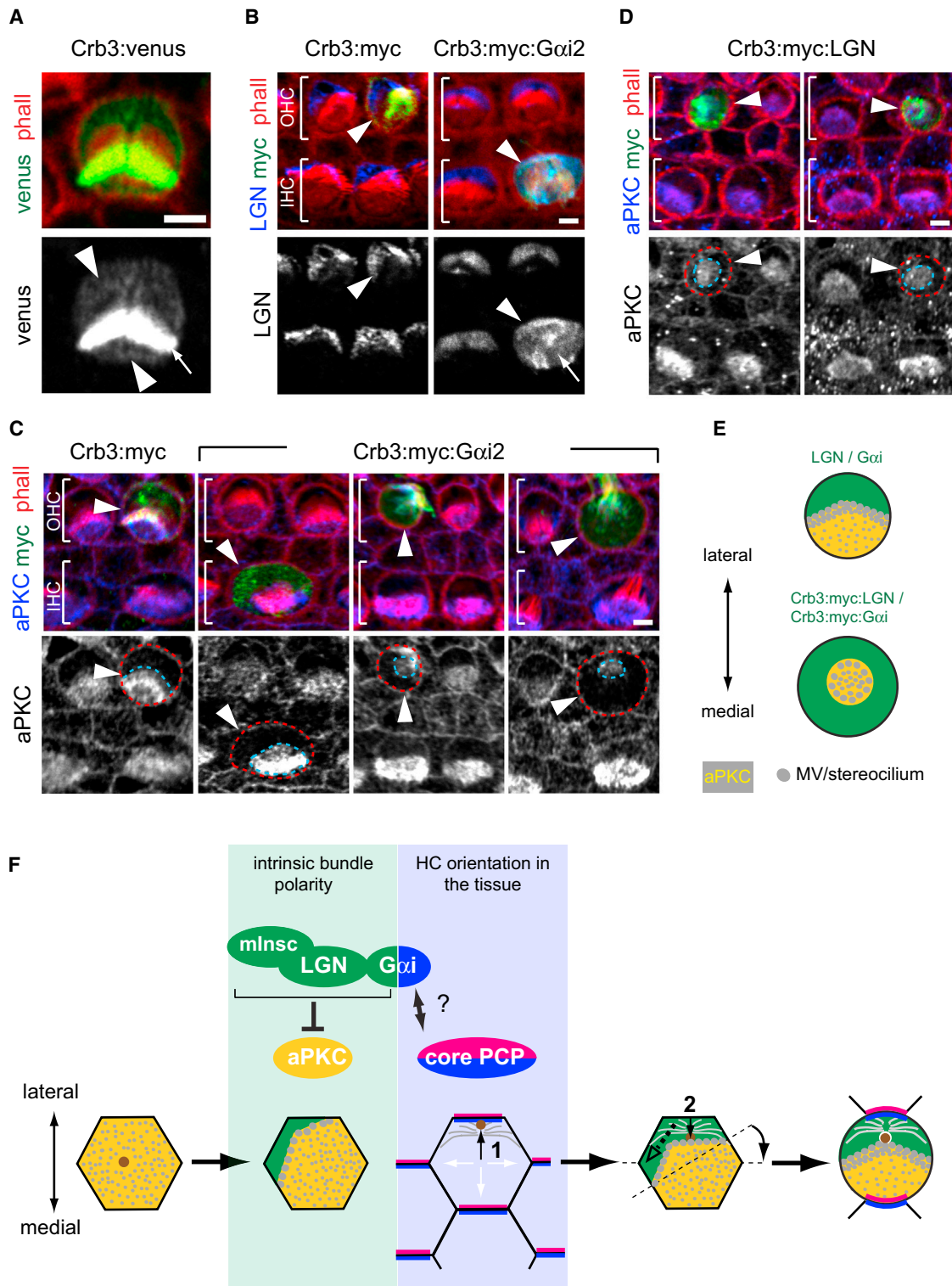


Figure 8. LGN/Gαi Negatively Regulates aPKC and Stereocilia Distribution to Shape the Bundle at the HC Apex

(A) A Crumbs3 (Crb3):venus fusion is enriched without planar asymmetry at the HC apex (arrowheads) and in the stereocilia bundle (arrow) in cochlea explants cultured for 6 days.

(B) Crb3:myc:Gαi, but not Crb3:myc delocalizes endogenous LGN to the whole HC apex (arrow). In (B–D), the electroporated HC (myc-positive, green) is indicated by arrowheads.

(C and D) Crb3:myc:Gαi (C) and Crb3:myc:LGN (D), but not Crb3:myc constrain aPKC and phalloidin-labeled microvilli/stereocilia to a central island at the HC apex (dotted blue circle). The electroporated HC boundary is shown by a dotted red circle.

(legend continued on next page)

Primary Antibodies

Primary antibodies used were rabbit anti-mInsc (raised against long isoform-specific MRRPPGDGDSTGEG peptide), rabbit anti-LGN (gifts from F. Matsuzaki, RIKEN, and Q. Du, Georgia Regents University), rabbit anti-Gxi (gift from J. Knoblich, IMBA), rabbit anti-pERM (gift from S. Carreno, Université de Montréal), rabbit anti-Par-3 (Upstate Biotechnology), rabbit or mouse anti-aPKC (SCBT), rabbit anti-phosphorylated aPKC (Cell Signaling Technology), mouse anti-acetylated α -tubulin (Sigma), rabbit anti-pericentrin (Covance), goat anti- γ -tubulin (SCBT), mouse anti-ZO-1 (Invitrogen), rabbit anti-Dvl2 (Cell Signaling Technology), goat anti-Fz6 (R&D Systems), rabbit anti-Egfp (Invitrogen), rabbit anti- β -galactosidase (Cappel), and mouse anti-myc (9e10, SCBT). Immunostainings were performed as described in the [Supplemental Experimental Procedures](#).

Cochlea Electroporation and Organotypic Culture

Cochlea electroporation and explant culture were carried out by modifying established protocols, as detailed in the [Supplemental Experimental Procedures](#). For all experiments, cochleas were electroporated at E14.5 and cultured for 6 days.

SUPPLEMENTAL INFORMATION

Supplemental Information includes Supplemental Experimental Procedures and eight figures and can be found with this article online at <http://dx.doi.org/10.1016/j.devcel.2013.09.011>.

ACKNOWLEDGMENTS

We thank F. Matsuzaki, Q. Du, J. Knoblich, and S. Carreno for antibodies; X. Morin for the PTXa construct; Q. Du for the Crb3:venus construct; M. Montcouquiol for advice on the cochlea explant procedure; and P. Gros for the Vangl2^{L^P} mouse line. We are grateful to J. Barthe for mouse colony maintenance, M. Cowan for help with ES cells, Q. Zhu for transgenic/knockout mouse production, E. Massicotte for cell sorting, and J. Chan and F. Charron for comments on the manuscript. This work was funded by a postdoctoral fellowship from the Human Frontier Science Program (to B.T.) and the Canadian Institutes of Health Research (grant number MOP-102584 to M.C.).

Received: March 20, 2013

Revised: August 29, 2013

Accepted: September 13, 2013

Published: October 14, 2013

REFERENCES

Afonso, C., and Henrique, D. (2006). PAR3 acts as a molecular organizer to define the apical domain of chick neuroepithelial cells. *J. Cell Sci.* **119**, 4293–4304.

Antic, D., Stubbs, J.L., Suyama, K., Kintner, C., Scott, M.P., and Axelrod, J.D. (2010). Planar cell polarity enables posterior localization of nodal cilia and left-right axis determination during mouse and *Xenopus* embryogenesis. *PLoS ONE* **5**, e8999.

Bergstralh, D.T., Lovegrove, H.E., and St Johnston, D. (2013). discs large links spindle orientation to apical-basal polarity in *Drosophila* epithelia. *Curr. Biol.* **23**, 1707–1712.

Borovina, A., Superina, S., Voskas, D., and Ciruna, B. (2010). Vangl2 directs the posterior tilting and asymmetric localization of motile primary cilia. *Nat. Cell Biol.* **12**, 407–412.

Cotanche, D.A., and Corwin, J.T. (1991). Stereociliary bundles reorient during hair cell development and regeneration in the chick cochlea. *Hear. Res.* **52**, 379–402.

Curtin, J.A., Quint, E., Tsipouri, V., Arkell, R.M., Cattanach, B., Copp, A.J., Henderson, D.J., Spurr, N., Stanier, P., Fisher, E.M., et al. (2003). Mutation of *Celsr1* disrupts planar polarity of inner ear hair cells and causes severe neural tube defects in the mouse. *Curr. Biol.* **13**, 1129–1133.

Deans, M.R., Antic, D., Suyama, K., Scott, M.P., Axelrod, J.D., and Goodrich, L.V. (2007). Asymmetric distribution of prickle-like 2 reveals an early underlying polarization of vestibular sensory epithelia in the inner ear. *J. Neurosci.* **27**, 3139–3147.

Denman-Johnson, K., and Forge, A. (1999). Establishment of hair bundle polarity and orientation in the developing vestibular system of the mouse. *J. Neurocytol.* **28**, 821–835.

Doherty, D., Chudley, A.E., Coghlan, G., Ishak, G.E., Innes, A.M., Lemire, E.G., Rogers, R.C., Mhanni, A.A., Phelps, I.G., Jones, S.J., et al.; FORGE Canada Consortium. (2012). GPSM2 mutations cause the brain malformations and hearing loss in Chudley-McCullough syndrome. *Am. J. Hum. Genet.* **90**, 1088–1093.

Du, Q., and Macara, I.G. (2004). Mammalian Pins is a conformational switch that links NuMA to heterotrimeric G proteins. *Cell* **119**, 503–516.

El-Hashash, A.H., Turcatel, G., Al Alam, D., Buckley, S., Tokumitsu, H., Bellusci, S., and Warburton, D. (2011). *Eya1* controls cell polarity, spindle orientation, cell fate and Notch signaling in distal embryonic lung epithelium. *Development* **138**, 1395–1407.

Goodrich, L.V., and Strutt, D. (2011). Principles of planar polarity in animal development. *Development* **138**, 1877–1892.

Guilgur, L.G., Prudêncio, P., Ferreira, T., Pimenta-Marques, A.R., and Martinho, R.G. (2012). *Drosophila* aPKC is required for mitotic spindle orientation during symmetric division of epithelial cells. *Development* **139**, 503–513.

Guirao, B., Meunier, A., Mortaud, S., Aguilar, A., Corsi, J.M., Strehl, L., Hirota, Y., Desoeuvre, A., Boutin, C., Han, Y.G., et al. (2010). Coupling between hydrodynamic forces and planar cell polarity orients mammalian motile cilia. *Nat. Cell Biol.* **12**, 341–350.

Hao, Y., Du, Q., Chen, X., Zheng, Z., Balsbaugh, J.L., Maitra, S., Shabanowitz, J., Hunt, D.F., and Macara, I.G. (2010). Par3 controls epithelial spindle orientation by aPKC-mediated phosphorylation of apical Pins. *Curr. Biol.* **20**, 1809–1818.

Hashimoto, M., Shinohara, K., Wang, J., Ikeuchi, S., Yoshida, S., Meno, C., Nonaka, S., Takada, S., Hatta, K., Wynshaw-Boris, A., and Hamada, H. (2010). Planar polarization of node cells determines the rotational axis of node cilia. *Nat. Cell Biol.* **12**, 170–176.

Izaki, T., Kamakura, S., Kohjima, M., and Sumimoto, H. (2006). Two forms of human Inscuteable-related protein that links Par3 to the Pins homologues LGN and AGS3. *Biochem. Biophys. Res. Commun.* **341**, 1001–1006.

Jones, C., Roper, V.C., Foucher, I., Qian, D., Banizs, B., Petit, C., Yoder, B.K., and Chen, P. (2008). Ciliary proteins link basal body polarization to planar cell polarity regulation. *Nat. Genet.* **40**, 69–77.

Kaltenbach, J.A., Falzarano, P.R., and Simpson, T.H. (1994). Postnatal development of the hamster cochlea. II. Growth and differentiation of stereocilia bundles. *J. Comp. Neurol.* **350**, 187–198.

Konno, D., Shioi, G., Shitamukai, A., Mori, A., Kiyonari, H., Miyata, T., and Matsuzaki, F. (2008). Neuroepithelial progenitors undergo LGN-dependent planar divisions to maintain self-renewability during mammalian neurogenesis. *Nat. Cell Biol.* **10**, 93–101.

Kraut, R., Chia, W., Jan, L.Y., Jan, Y.N., and Knoblich, J.A. (1996). Role of inscuteable in orienting asymmetric cell divisions in *Drosophila*. *Nature* **383**, 50–55.

Lu, X.W., Borchers, A.G.M., Jolicoeur, C., Rayburn, H., Baker, J.C., and Tessier-Lavigne, M. (2004). PTK7/CCK-4 is a novel regulator of planar cell polarity in vertebrates. *Nature* **430**, 93–98.

(E) Schematic representation of normal (top) and delocalized (bottom) LGN/Gxi influence on aPKC and microvilli/stereocilia distribution.

(F) Model depicting how intrinsic HC bundle polarity (regulated by mInsc/LGN/Gxi and aPKC polarized at the AS) and HC orientation in the field (regulated by core PCP proteins polarized at apical junctions and Gxi) could be coordinated in time. Arrows “1” and “2” depict the early shift and subsequent inward relocalization of the kinocilium, respectively. See [Discussion](#) for details. MV, microvillus. Scale bars: 2 μ m. See also [Figure S8](#).

- Martin-Belmonte, F., Gassama, A., Datta, A., Yu, W., Rescher, U., Gerke, V., and Mostov, K. (2007). PTEN-mediated apical segregation of phosphoinositides controls epithelial morphogenesis through Cdc42. *Cell* 128, 383–397.
- McKenzie, E., Krupin, A., and Kelley, M.W. (2004). Cellular growth and rearrangement during the development of the mammalian organ of Corti. *Dev. Dyn.* 229, 802–812.
- Mitchell, B., Stubbs, J.L., Huisman, F., Taborek, P., Yu, C., and Kintner, C. (2009). The PCP pathway instructs the planar orientation of ciliated cells in the *Xenopus* larval skin. *Curr. Biol.* 19, 924–929.
- Montcouquiol, M., Rachel, R.A., Lanford, P.J., Copeland, N.G., Jenkins, N.A., and Kelley, M.W. (2003). Identification of *Vangl2* and *Scrb1* as planar polarity genes in mammals. *Nature* 423, 173–177.
- Montcouquiol, M., Sans, N., Huss, D., Kach, J., Dickman, J.D., Forge, A., Rachel, R.A., Copeland, N.G., Jenkins, N.A., Bogani, D., et al. (2006). Asymmetric localization of *Vangl2* and *Fz3* indicate novel mechanisms for planar cell polarity in mammals. *J. Neurosci.* 26, 5265–5275.
- Morais-de-Sá, E., Mirouse, V., and St Johnston, D. (2010). aPKC phosphorylation of Bazooka defines the apical/lateral border in *Drosophila* epithelial cells. *Cell* 141, 509–523.
- Morin, X., and Bellaïche, Y. (2011). Mitotic spindle orientation in asymmetric and symmetric cell divisions during animal development. *Dev. Cell* 27, 102–119.
- Morin, X., Jaouen, F., and Durbec, P. (2007). Control of planar divisions by the G-protein regulator LGN maintains progenitors in the chick neuroepithelium. *Nat. Neurosci.* 10, 1440–1448.
- Parmentier, M.L., Woods, D., Greig, S., Phan, P.G., Radovic, A., Bryant, P., and O’Kane, C.J. (2000). Rapsynoid/partner of inscuteable controls asymmetric division of larval neuroblasts in *Drosophila*. *J. Neurosci.* 20, RC84.
- Peyre, E., Jaouen, F., Saadaoui, M., Haren, L., Merdes, A., Durbec, P., and Morin, X. (2011). A lateral belt of cortical LGN and NuMA guides mitotic spindle movements and planar division in neuroepithelial cells. *J. Cell Biol.* 193, 141–154.
- Postiglione, M.P., Jüschke, C., Xie, Y., Haas, G.A., Charalambous, C., and Knoblich, J.A. (2011). Mouse inscuteable induces apical-basal spindle orientation to facilitate intermediate progenitor generation in the developing neocortex. *Neuron* 72, 269–284.
- Poulson, N.D., and Lechler, T. (2010). Robust control of mitotic spindle orientation in the developing epidermis. *J. Cell Biol.* 191, 915–922.
- Richardson, G.P., de Monvel, J.B., and Petit, C. (2011). How the genetics of deafness illuminates auditory physiology. *Annu. Rev. Physiol.* 73, 311–334.
- Saotome, I., Curto, M., and McClatchey, A.I. (2004). Ezrin is essential for epithelial organization and villus morphogenesis in the developing intestine. *Dev. Cell* 6, 855–864.
- Schaefer, M., Shevchenko, A., Shevchenko, A., and Knoblich, J.A. (2000). A protein complex containing Inscuteable and the Galpha-binding protein Pins orients asymmetric cell divisions in *Drosophila*. *Curr. Biol.* 10, 353–362.
- Schaefer, M., Petronczki, M., Dorner, D., Forte, M., and Knoblich, J.A. (2001). Heterotrimeric G proteins direct two modes of asymmetric cell division in the *Drosophila* nervous system. *Cell* 107, 183–194.
- Schober, M., Schaefer, M., and Knoblich, J.A. (1999). Bazooka recruits Inscuteable to orient asymmetric cell divisions in *Drosophila* neuroblasts. *Nature* 402, 548–551.
- Shotwell, S.L., Jacobs, R., and Hudspeth, A.J. (1981). Directional sensitivity of individual vertebrate hair cells to controlled deflection of their hair bundles. *Ann. N Y Acad. Sci.* 374, 1–10.
- Sipe, C.W., and Lu, X. (2011). Kif3a regulates planar polarization of auditory hair cells through both ciliary and non-ciliary mechanisms. *Development* 138, 3441–3449.
- Song, H., Hu, J., Chen, W., Elliott, G., Andre, P., Gao, B., and Yang, Y. (2010). Planar cell polarity breaks bilateral symmetry by controlling ciliary positioning. *Nature* 466, 378–382.
- Tilney, L.G., Tilney, M.S., and DeRosier, D.J. (1992). Actin filaments, stereocilia, and hair cells: how cells count and measure. *Annu. Rev. Cell Biol.* 8, 257–274.
- Tissir, F., Qu, Y., Montcouquiol, M., Zhou, L., Komatsu, K., Shi, D., Fujimori, T., Labeau, J., Tyteca, D., Courtoy, P., et al. (2010). Lack of cadherins *Celsr2* and *Celsr3* impairs ependymal ciliogenesis, leading to fatal hydrocephalus. *Nat. Neurosci.* 13, 700–707.
- Vladar, E.K., Bayly, R.D., Sangoram, A.M., Scott, M.P., and Axelrod, J.D. (2012). Microtubules enable the planar cell polarity of airway cilia. *Curr. Biol.* 22, 2203–2212.
- Wald, F.A., Oriolo, A.S., Mashukova, A., Fregien, N.L., Langshaw, A.H., and Salas, P.J. (2008). Atypical protein kinase C (iota) activates ezrin in the apical domain of intestinal epithelial cells. *J. Cell Sci.* 121, 644–654.
- Walsh, T., Shahin, H., Elkan-Miller, T., Lee, M.K., Thornton, A.M., Roeb, W., Abu Rayyan, A., Loulus, S., Avraham, K.B., King, M.C., and Kanaan, M. (2010). Whole exome sequencing and homozygosity mapping identify mutation in the cell polarity protein *GPSM2* as the cause of nonsyndromic hearing loss DFNB82. *Am. J. Hum. Genet.* 87, 90–94.
- Walther, R.F., and Pichaud, F. (2010). Crumbs/DaPKC-dependent apical exclusion of Bazooka promotes photoreceptor polarity remodeling. *Curr. Biol.* 20, 1065–1074.
- Wang, J., Mark, S., Zhang, X., Qian, D., Yoo, S.J., Radde-Gallwitz, K., Zhang, Y., Lin, X., Collazo, A., Wynshaw-Boris, A., and Chen, P. (2005). Regulation of polarized extension and planar cell polarity in the cochlea by the vertebrate PCP pathway. *Nat. Genet.* 37, 980–985.
- Wang, Y., Guo, N., and Nathans, J. (2006). The role of *Frizzled3* and *Frizzled6* in neural tube closure and in the planar polarity of inner-ear sensory hair cells. *J. Neurosci.* 26, 2147–2156.
- Williams, S.E., Beronja, S., Pasolli, H.A., and Fuchs, E. (2011). Asymmetric cell divisions promote Notch-dependent epidermal differentiation. *Nature* 470, 353–358.
- Wodarz, A., Ramrath, A., Kuchinke, U., and Knust, E. (1999). Bazooka provides an apical cue for Inscuteable localization in *Drosophila* neuroblasts. *Nature* 402, 544–547.
- Wodarz, A., Ramrath, A., Grimm, A., and Knust, E. (2000). *Drosophila* atypical protein kinase C associates with Bazooka and controls polarity of epithelia and neuroblasts. *J. Cell Biol.* 150, 1361–1374.
- Wong, L.L., and Adler, P.N. (1993). Tissue polarity genes of *Drosophila* regulate the subcellular location for prehair initiation in pupal wing cells. *J. Cell Biol.* 123, 209–221.
- Yariz, K.O., Walsh, T., Akay, H., Duman, D., Akkaynak, A.C., King, M.C., and Tekin, M. (2012). A truncating mutation in *GPSM2* is associated with recessive non-syndromic hearing loss. *Clin. Genet.* 81, 289–293.
- Yu, F., Morin, X., Cai, Y., Yang, X., and Chia, W. (2000). Analysis of partner of inscuteable, a novel player of *Drosophila* asymmetric divisions, reveals two distinct steps in inscuteable apical localization. *Cell* 100, 399–409.
- Yuzawa, S., Kamakura, S., Iwakiri, Y., Hayase, J., and Sumimoto, H. (2011). Structural basis for interaction between the conserved cell polarity proteins Inscuteable and Leu-Gly-Asn repeat-enriched protein (LGN). *Proc. Natl. Acad. Sci. USA* 108, 19210–19215.
- Zheng, Z., Zhu, H., Wan, Q., Liu, J., Xiao, Z., Siderovski, D.P., and Du, Q. (2010). LGN regulates mitotic spindle orientation during epithelial morphogenesis. *J. Cell Biol.* 189, 275–288.
- Zhu, J., Wen, W., Zheng, Z., Shang, Y., Wei, Z., Xiao, Z., Pan, Z., Du, Q., Wang, W., and Zhang, M. (2011). LGN/mlnsc and LGN/NuMA complex structures suggest distinct functions in asymmetric cell division for the Par3/mlnsc/LGN and *Gxi*/LGN/NuMA pathways. *Mol. Cell* 43, 418–431.
- Zigman, M., Cayouette, M., Charalambous, C., Schleiffer, A., Hoeller, O., Dunican, D., McCudden, C.R., Firnberg, N., Bares, B.A., Siderovski, D.P., and Knoblich, J.A. (2005). Mammalian inscuteable regulates spindle orientation and cell fate in the developing retina. *Neuron* 48, 539–545.
- Zine, A., and Romand, R. (1996). Development of the auditory receptors of the rat: a SEM study. *Brain Res.* 721, 49–58.